OPEN ACCESS
CellPress

Cell Reports
Article

EZH2-Mediated Inactivation of IFN-γ-JAK-STAT1 Signaling Is an Effective Therapeutic Target in MYC-Driven Prostate Cancer

Zhen Ning Wee,[1,3] Zhimei Li,[1] Puay Leng Lee,[1] Shuet Theng Lee,[1] Yoon Pin Lim,[2,3] and Qiang Yu[1,4,5,*]
[1]Cancer Therapeutics & Stratified Oncology, Genome Institute of Singapore, Agency for Science, Technology, and Research (A*STAR), Biopolis, Singapore 138672, Singapore
[2]Department of Biochemistry, Yong Loo Lin School of Medicine, National University of Singapore, Singapore 117599, Singapore
[3]NUS Graduate School for Integrative Sciences and Engineering, National University of Singapore, Singapore 117456, Singapore
[4]Department of Physiology, Yong Loo Lin School of Medicine, National University of Singapore, Singapore 117597, Singapore
[5]Cancer and Stem Cell Biology, DUKE-NUS Graduate Medical School of Singapore, Singapore 169857, Singapore
*Correspondence: yuq@gis.a-star.edu.sg
http://dx.doi.org/10.1016/j.celrep.2014.05.045

SUMMARY

Although small-molecule targeting of EZH2 appears to be effective in lymphomas carrying EZH2 activating mutations, finding similar approaches to target EZH2-overexpressing epithelial tumors remains challenging. In MYC-driven, but not PI3K-driven prostate cancer, we show that interferon-γ receptor 1 (IFNGR1) is directly repressed by EZH2 in a MYC-dependent manner and is downregulated in a subset of metastatic prostate cancers. EZH2 knockdown restored the expression of IFNGR1 and, when combined with IFN-γ treatment, led to strong activation of IFN-JAK-STAT1 tumor-suppressor signaling and robust apoptosis. Pharmacologic depletion of EZH2 by the histone-methylation inhibitor DZNep mimicked the effects of EZH2 knockdown on IFNGR1 induction and delivered a remarkable synergistic antitumor effect with IFN-γ. In contrast, although they efficiently depleted histone Lysine 27 trimethylation, EZH2 catalytic inhibitors failed to mimic EZH2 depletion. Thus, EZH2-inactivated IFN signaling may represent a therapeutic target, and patients with advanced prostate cancer driven by MYC may benefit from the combination of EZH2 and IFN-γ-targeted therapy.

INTRODUCTION

Polycomb repressor complex 2 (PRC2) is an important regulator of cell growth, survival, and differentiation (Margueron and Reinberg, 2011). Pathologic activation of one of its enzymatic components, EZH2 histone methyltransferase, through either overexpression (Bracken et al., 2003; Kleer et al., 2003; Varambally et al., 2002) or activating mutations (McCabe et al., 2012a; Morin et al., 2010; Nikoloski et al., 2010; Sneeringer et al., 2010; Yap et al., 2011) is among the most common genetic alterations observed in human cancers and plays a crucial role in disease progression by deregulating the transcriptional program, which influences cell growth (Bracken et al., 2003; Bryant et al., 2007; Qi et al., 2012), survival (Varambally et al., 2002), invasion (Bracken et al., 2003; Bryant et al., 2007), and metastasis (Bachmann et al., 2006; Ren et al., 2012; Varambally et al., 2002). Validation of EZH2 as a therapeutic target is supported by numerous lines of experimental evidence (Gonzalez et al., 2009; Melnick, 2012; Popovic and Licht, 2012). As a key component of PRC2, EZH2 mediates trimethylation on histone 3 lysine 27 (H3K27me3) and gene silencing, which have been recognized as key mechanisms that contribute to oncogenesis (Chang and Hung, 2012; Margueron and Reinberg, 2011). This seems to be true particularly in non-Hodgkin's lymphoma cells that carry EZH2-activating mutations leading to hyper H3K27me3, as small-molecule inhibitors targeting EZH2-mediated H3K27me3 are sufficient to induce loss of viability of these cells (Knutson et al., 2012; McCabe et al., 2012b; Qi et al., 2012). However, although these EZH2 catalytic inhibitors deplete H3K27me3 robustly, they do not seem to be potent in solid tumor cells (Kim et al., 2013b). Thus, there is a continuing demand for a potent therapeutic approach to target the majority of human epithelial cancers in which EZH2 is often overexpressed but not mutated.

Although a variety of EZH2 target genes have been identified in various cancers (Cao et al., 2008; Kodach et al., 2010; Li et al., 2012; Yu et al., 2007, 2010), a whole-genome analysis indicated that EZH2-silenced genes appear to be moving targets and vary from cancer to cancer (Kondo et al., 2008). An EZH2 target common to multiple cancers with both functional and therapeutic implications has not been described to date. The absence of such an EZH2 target has created a formidable obstacle against the development of a biomarker strategy to guide EZH2-targeted therapy that can be applied more generally in human cancers.

In this study, we report that Interferon γ Receptor 1 (*IFNGR1*) is a target that is directly silenced by EZH2 in MYC-driven prostate cancer cells. EZH2 inhibition, either by genetic knockdown or by pharmacologic depletion, restores the expression of *IFNGR* and

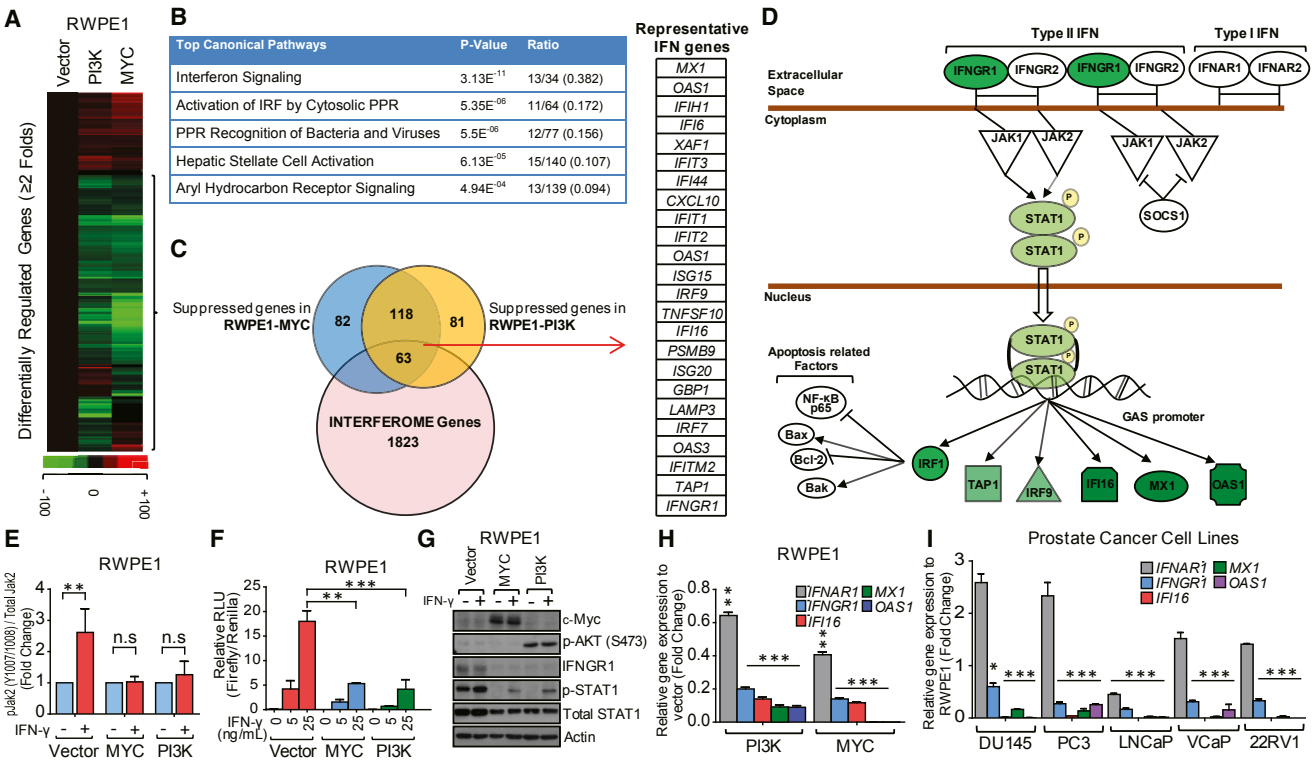

Figure 1. Oncogenic Transformation by MYC- and PI3K-Induced Transcriptional Inactivation of the IFN-γ-JAK-STAT1 Signaling Pathway

(A) Unsupervised hierarchical clustering showing 610 genes that were differentially regulated in either RWPE1-MYC or RWPE1-PI3K cells compared with RWPE1-vector control cells (2-fold cutoff, $p < 0.01$). The colored scale bar represents the absolute fold change.

(B) IPA showing the IFN signaling pathway as the top gene network enriched in downregulated genes in transformed RWPE1 cells.

(C) Venn diagram (not drawn to scale) showing the overlapping of genes downregulated in RWPE1-MYC and RWPE1-PI3K cells with known IFN genes in the Interferome database.

(D) Graphical depiction of representative IFN genes in the IFN-JAK-STAT1 pathway. Green molecules represent those that were downregulated.

(E) ELISA showing JAK2 phosphorylation and activation in RWPE cells treated with or without IFN-γ. The Y1007/1008 phosphorylation level of JAK2 was normalized and expressed as the fold change against the total JAK2 level. Sensitivity to IFN-γ was determined by comparing the phosphorylation status of JAK2 between IFN-γ-treated and untreated control cells.

(F) STAT1-driven luciferase reporter activity of indicated RWPE1 cell lines treated with or without IFN-γ.

(G) Western blotting showing the IFNGR1 and STAT1 phosphorylation in RWPE1 cell lines treated with or without IFN-γ.

(H and I) qRT-PCR analysis of *IFNGR1* and multiple IFN genes in (H) RWPE1-MYC and RWPE1-PI3K cells, as well as (I) prostate cancer cell lines normalized to RWPE1 control counterparts.

All the data in the graph bars represent mean + SEM, n = 3. $^{**}p < 0.01$, $^{***}p < 0.001$, n.s., not significant.

See also Figure S1 and Table S1.

thus activation of IFN-JAK-STAT1 signaling, leading to robust antitumor effects in response to interferon γ (IFN-γ) treatment. These results indicate that pharmacologic targeting of EZH2 in combination with IFN-γ may provide a treatment strategy for advanced prostate cancers.

RESULTS

MYC- or PI3K-Mediated Oncogenic Transformation in Prostate Epithelial Cells Induces Transcriptional Inactivation of IFN-γ-JAK-STAT1 Signaling

Gene amplification of MYC or constitutive activation of the PI3K signaling pathway occurs frequently in advanced prostate cancer (Gurel et al., 2008; Jenkins et al., 1997; Majumder and Sellers, 2005; Sato et al., 1999). To investigate the molecular events induced by MYC or PI3K, we used immortalized prostate epithelial RWPE cells and infected them with retroviral *MYC* or a constitutively activating mutant of *PIK3CA* (E545K), resulting in transformed cell lines that showed elevated levels of MYC or AKT phosphorylation, designated as RWPE1-MYC and RWPE1-PI3K, respectively (see Figures S1 and 2C). Because oncogenic transformation is often coupled with epigenetic gene silencing (Gazin et al., 2007), we performed gene-expressing profiling and focused on pathways and gene sets that are downregulated upon oncogenic transformation. Among 610 genes that were differentially expressed (with a 2-fold cutoff, $p < 0.01$), we identified a set of 344 genes that were downregulated in both RWPE1-MYC and RWPE1-PI3K cells as compared with the empty vector control RWPE1 cells (Figure 1A; Table S1). An ingenuity pathway analysis (IPA) indicated that this gene set

was enriched for canonical IFN signaling as the top gene network ($p < 3 \times 10^{-11}$) (Figure 1B). Furthermore, 63 out of 344 genes commonly downregulated in MYC- and PI3K-activated cell lines were identified as IFN-responsive genes (IFN genes) in the Interferome database (Figure 1C), which can be mapped at multiple levels in the IFN-JAK-STAT1 signaling cascade (Figure 1D, highlighted in green). Notably, *IFNGR1*, which encodes IFNGR1, was downregulated, whereas *IFNAR1*, which encodes IFN α1 receptor (IFNAR1), was not (Figure 1D). Thus, these findings suggest that MYC or PI3K activation in prostate epithelial cells may have induced a transcriptional inactivation of IFN signaling, which is specific for *IFNGR1*, but not *IFNAR1*.

Downregulation of *IFNGR1* expression is expected to cause a reduced response to IFN-γ stimulation, leading to impaired activation of JAK-STAT1 activity. Indeed, IFN-γ-induced phosphorylation of JAK2 and STAT1 transcriptional activity, as measured by an ELISA-based assay and a STAT1-mediated luciferase reporter assay, respectively, were much reduced in both RWPE1-MYC and RWPE1-PI3K cells as compared with the control RWPE1 cells (Figures 1E and 1F). Consistently, western blotting confirmed the downregulation of IFNGR1 protein expression and dampened induction of STAT1 Tyr701 phosphorylation in response to IFN-γ treatment in RWPE1-MYC and RWPE1-PI3K cells as compared with the RWPE1 cells (Figure 1G). A quantitative RT-PCR (qRT-PCR) analysis further validated the gene-expression array data by showing the downregulation of *IFNGR1* and various *IFN* downstream genes in both MYC- and PI3K-transformed RWPE1 cells (Figure 1H). Importantly, the downregulation of *IFNGR1* (but not *IFNAR1*) and the downstream *IFN*-responsive genes was also found in a panel of prostate cancer cell lines (Figure 1I).

IFNGR1 Is a Direct Target of EZH2 in MYC-Driven, but Not PI3K-Driven, Prostate Cancer Cells

The mechanism of loss of *IFNGR1* and its downstream IFN-responsive genes could result from epigenetic modifications such as DNA methylation or histone modifications. Given the well-known role of EZH2 in advanced prostate cancer (Varambally et al., 2002), and that both *MYC* and PI3K signaling pathways were recently shown to regulate EZH2 expression or activity (Cha et al., 2005; Koh et al., 2011; Sander et al., 2008), we investigated a possible role of EZH2 in controlling IFN signaling in *MYC*- and *PI3K*-transformed cells. We found that the ectopic overexpression of EZH2 in RWPE1 cells was able to selectively downregulate *IFNGR1* (but not *IFNAR1*) and other IFN-responsive genes (Figure 2A). Notably, in RWPE1-MYC cells, *EZH2* knockdown was able to restore the expression of *IFNGR1* (but not *IFNAR1*); however, this was not seen in RWPE1-PI3K cells (Figure 2B). Thus, EZH2 appears to be involved in *IFNGR1* repression only in MYC-driven cells, and not in PI3K-driven cells.

MYC is known to upregulate EZH2 expression by downregulating miR-26a/b (Koh et al., 2011; Sander et al., 2008). It has also been shown to affect EZH2 activity by antagonizing PI3K-AKT-mediated phosphorylation of EZH2 on serine 21 (Cha et al., 2005; Kaur and Cole, 2013). Akt-induced EZH2 phosphorylation on serine 21 is inhibitory to EZH2 gene-silencing activity (Cha et al., 2005) but promotes its Polycomb-independent oncogenic activity (Kim et al., 2013a; Xu et al., 2012). Indeed, we found that MYC-driven RWPE cells showed concurrent reductions of phosphorylation on both AKT (S473) and EZH2 (S21) as compared with PI3K-driven cells (Figure 2C). Meanwhile, MYC overexpression led to only a modest decrease in miR-26a, and consistently a modest induction of EZH2 mRNA (Figures S2A and S2B). These findings suggest that MYC overexpression in our system more likely modulates the EZH2 activity by counteracting AKT-mediated EZH2 inhibition, rather than through a miR-26a-mediated mechanism.

Next, we investigated whether EZH2 directly represses *IFNGR1* as well as the downstream IFN genes. Chromatin immunoprecipitation (ChIP) followed by qPCR analysis in the vicinity of the promoter region of *IFNGR1* (Figure 2D) showed a significant EZH2 enrichment in RWPE1-MYC cells (Figure 2E) compared with the positive control gene (*CNR1*), but not in RWPE1-PI3K or the vector control RWPE cells (Figure 2E). In addition, no EZH2 enrichment was found in genes downstream of *IFNGR1* (Figure S2C). Therefore, the transcriptional inactivation of IFN-JAK-STAT1 signaling seen in MYC-driven cells may stem from a direct suppression of *IFNGR1* by EZH2.

Similar to what we observed in transformed RWPE1-MYC cells, we found a significant EZH2 enrichment in the *IFNGR1* promoter of two prostate cancer cell lines, DU145 and PC3, which have been reported to carry MYC amplification or sensitivity to MYC inhibition (Luoto et al., 2010; Supino et al., 2007), but not in LNCaP and 22RV1 cells, which are less sensitive to MYC knockdown and thus appear to be MYC independent (Figures 2F and S2D). Furthermore, *MYC* knockdown in DU145 cells resulted in a much reduced enrichment of both EZH2 and H3K27me3 at the *IFNGR1* promoter (Figure 2G), but this was not seen in LNCaP cells. These data further support the notion that EZH2-mediated silencing of *IFNGR1* is MYC-dependent.

In addition, we found partial DNA hypermethylation in the *IFNGR1* promoter in RWPE1-PI3K cells and LNCaP cells, but not in RWPE1-MYC and DU145 cells (Figure S2E). Thus, based on the results we obtained from both transformed RWPE1 cells and prostate cancer cell lines, we conclude that EZH2-mediated repression of *IFNGR1* is restricted to MYC-associated prostate cancer cells, whereas *IFNGR1* downregulation in PI3K-transformed RWPE1 or LNCaP cells is independent of EZH2 and might be associated with the promoter DNA hypermethylation.

IFNGR1 Is Downregulated in a Subset of Metastatic Prostate Tumors Associated with *MYC*

To validate the *IFNGR1* downregulation observed in clinical samples, we examined the expression of *IFNGR1*, as well as *MYC* and *EZH2*, in a previously published prostate cancer gene-expression data set that covers the disease progression from benign prostatic epithelium to metastatic prostate cancer (Jenkins et al., 1997; Varambally et al., 2002; Wolfer et al., 2010). We found that a subset of metastatic tumors showed a strong upregulation of *MYC* and *EZH2*, whereas *IFNGR1* and the downstream IFN genes were downregulated toward the metastatic progression (Figure 3A). Moreover, when we stratified these tumors based on the *MYC* levels, we found that high *MYC* tumors tended to express higher levels of *EZH2* and lower levels of *IFNGR1* (Figure 3B).

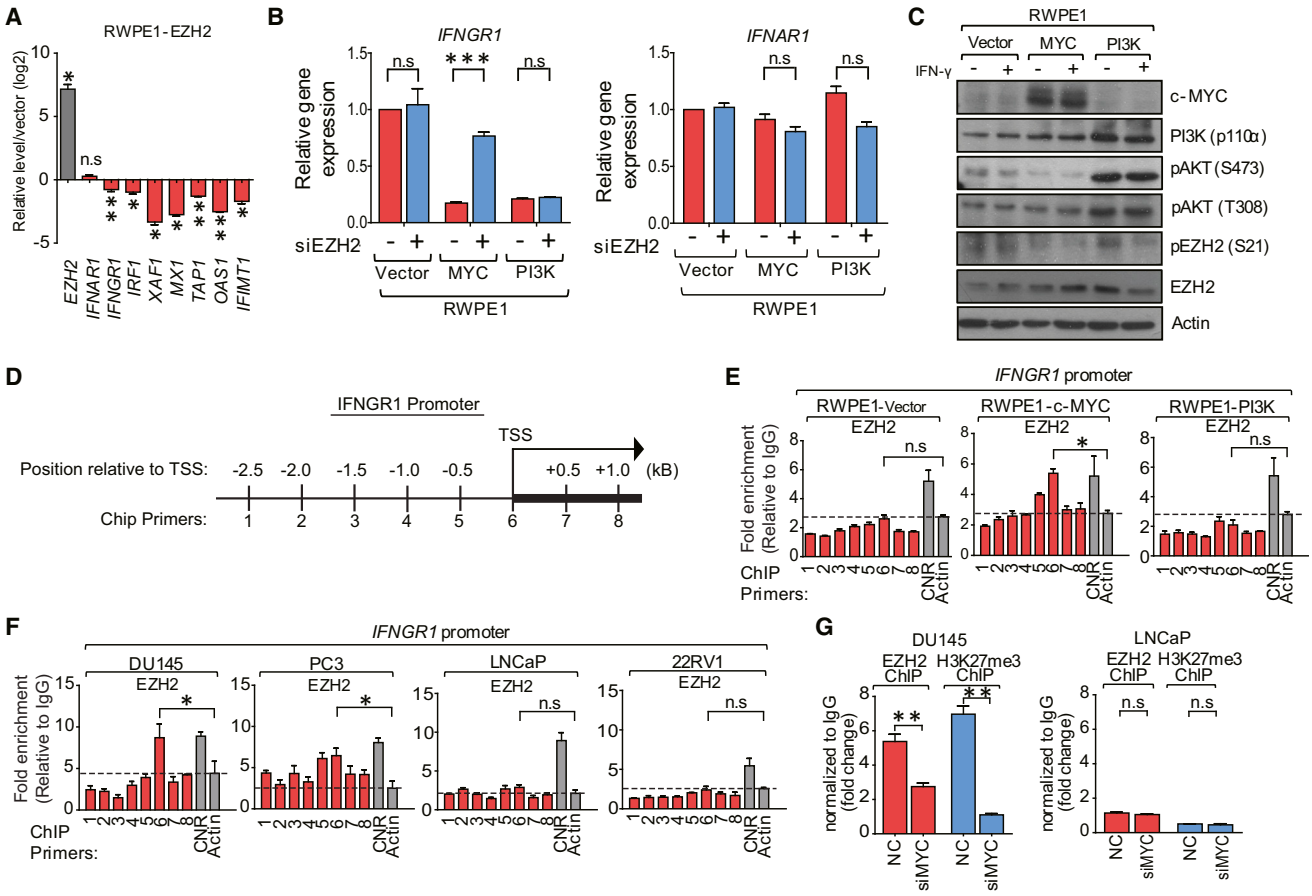

Figure 2. *IFNGR1* Is a Direct Target of EZH2 in MYC-Driven, but Not PI3K-Driven, Prostate Cancer Cells

(A) qRT-PCR analysis of *IFNGR1* and other IFN genes upon ectopic EZH2 expression in RWPE1 cells.

(B) qRT-PCR showing the restoration of *IFNGR1*, but not *IFNAR1*, expression following EZH2 knockdown in RWPE1-MYC, but not RWPE1-PI3K, cells.

(C) Western blotting validating the overexpression of c-MYC and the constitutive active mutant of PI3K, and the phosphorylation status of AKT and EZH2 in RWPE1 cell lines treated with or without IFN-γ.

(D) Schematic showing the ChIP primer locations with respect to the transcriptional start site (TSS) of the *IFNGR1* promoter.

(E) ChIP analysis showing the enrichment of EZH2 at the promoter of *IFNGR1* in transformed cell lines as indicated. Shown are the fold enrichments over the immunoglobulin G (IgG) control further normalized to the *Actin* promoter. The *CNR* gene is a known target gene of EZH2. Hence, the promoter region of *CNR* was used as a positive control for the detection of EZH2 binding.

(F) ChIP analysis of EZH2 enrichment at the promoter of *IFNGR1* in the indicated prostate cancer cell lines.

(G) ChIP analysis showing the enrichment of EZH2 and H3K27me3 in the *IFNGR1* promoter in DU145 and LNCaP cells before and after MYC knockdown.

All data in the graph bars represent mean + SEM, n = 3. *p < 0.05, **p < 0.01, ***p < 0.001, n.s., not significant. See also Figure S2.

Immunohistochemistry (IHC) analysis of a tissue microarray (TMA) consisting of a set of 80 prostate tissues of different grades and stages confirmed that higher MYC protein levels were associated with higher EZH2 but lower IFNGR1 protein expression (Figure 3C). Moreover, IFNGR1 was expressed in much lower levels in high-grade advanced prostate tumors as compared with low-grade tumors (Figure 3D). Among the high-grade tumors, approximately one-third of the tumors had higher MYC and EZH2 protein levels, which were negatively correlated with the expression of IFNGR1 in these tumors (Figure 3E), as shown in a set of representative tumors in different stages (Figure 3F). Thus, our findings suggest that IFNGR1 downregulation by EZH2 may occur in a subset (~30%) of advanced prostate tumors associated with MYC.

EZH2-Mediated Inactivation of IFN-γ-JAK-STAT1 Signaling Pathway Confers Growth and Survival Advantages in MYC-Dependent Prostate Cancer Cells

Activation of IFN-γ-STAT1 signaling is known to be tumor suppressive through the induction of a number of IFN-responsive genes, including the apoptosis-promoting *IRF1* (Park et al., 2004). Loss of *IFNGR1* expression by EZH2 is expected to cause a reduced sensitivity to IFN-γ treatment, resulting in defective activation of JAK-STAT1 signaling and its downstream target genes. Consistent with this hypothesis, *EZH2* knockdown resulted in robust activation of IFN genes in response to IFN-γ stimulation in MYC-dependent DU145 and PC3 cells, but not in MYC-independent LNCap and 22RV1 cells (Figure 4A). Consistently, *EZH2* knockdown in DU145 cells restored IFNGR1

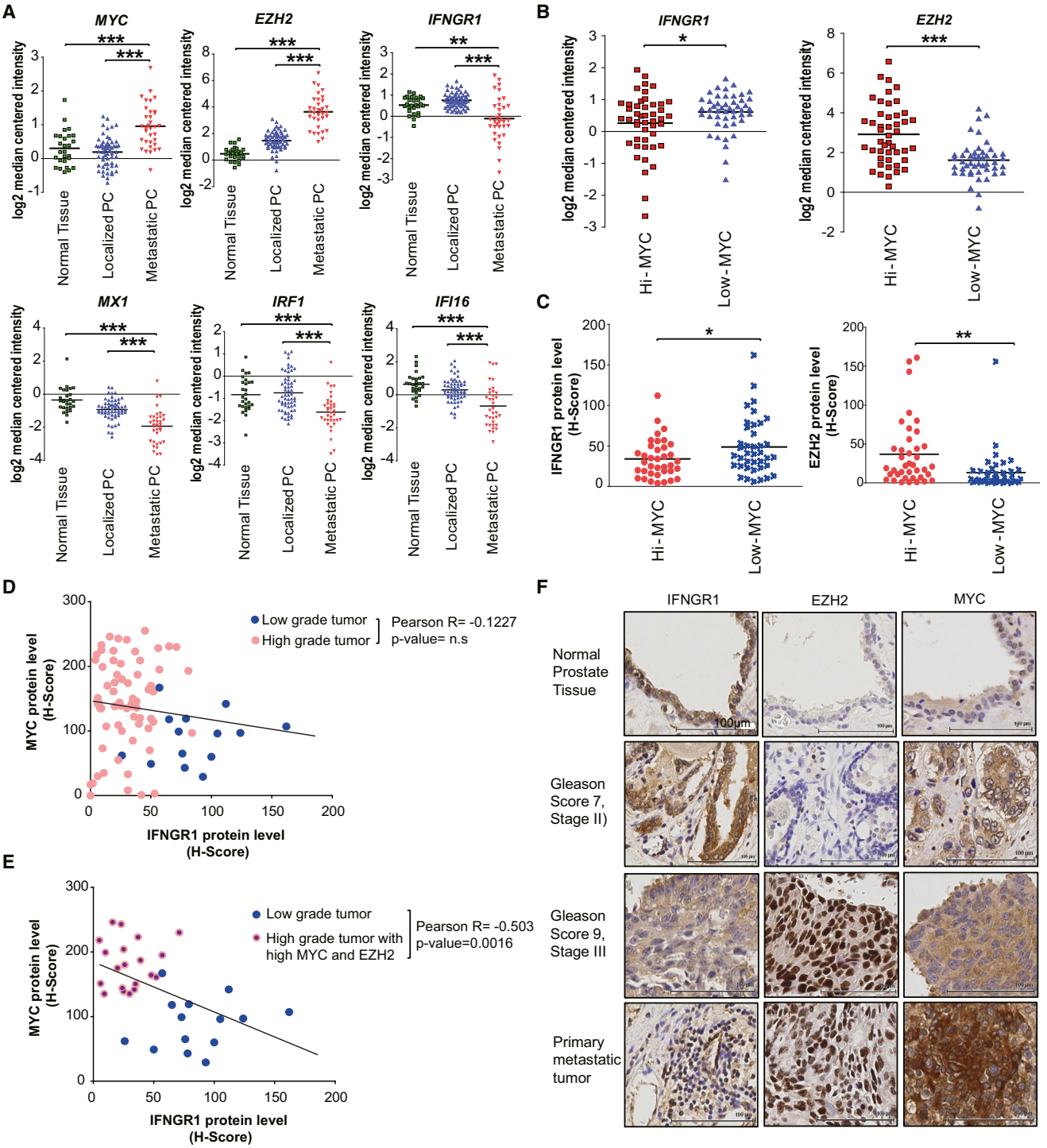

Figure 3. Inverse Relationship between *MYC*/*EZH2* and *IFNGR1* Expression Levels in Advanced Prostate Cancer

(A) Scatterplot showing the mRNA expression (Log_2) of *EZH2*, *MYC*, *IFNGR1*, and IFN-γ responsive genes (*MX1*, *IRF1*, and *IFI16*), comparing metastatic (n = 35) and localized (n = 59) prostate tumors with normal prostate tissue (n = 28) from the Grasso Prostate data set (Grasso et al., 2012).

(B) Scatterplot showing the mRNA expression (Log_2) of *IFNGR1* (left) and *EZH2* (right) after stratifying all prostate cancer tumors in the Grasso Prostate data set according to their *MYC* expression. Prostate tumors with *MYC* expression higher or lower than the median level were categorized as the "Hi-*MYC*" (n = 59) or "Low-*MYC*" (n = 61) group, respectively.

(C) IFNGR1 (left) and EZH2 (right) protein expression of the TMA performed in (C) as represented by the H-score. The prostate tumors are stratified into "Hi-MYC" (n = 39) and "Low-MYC" (n = 41) groups according to their MYC protein expression in a fashion similar to that described in (B).

(legend continued on next page)

protein expression and enhanced STAT1 phosphorylation and the expression of IFI16, a downstream target gene of STAT1 (Figure 4B), as well as JAK2 phosphorylation in response to IFN-γ stimulation (Figure 4C). Consistent with MYC being upstream of EZH2 (Kaur and Cole, 2013; Koh et al., 2011; Sander et al., 2008), *MYC* knockdown in DU145 cells resulted in decreased EZH2 expression, which gave rise to a similar increase in *IFNGR1* expression and STAT1 activation in response to IFN-γ stimulation (Figure 4D).

Phenotypically, either *MYC* or *EZH2* knockdown, when combined with IFN-γ treatment, resulted in remarkable synergy in cell-growth regression in MYC-dependent DU145 cells, indicating an induction of cell death (Figure 4E, top). By contrast, such an effect was not observed in MYC-independent LNCaP cells (Figure 4E, bottom). Further assessment of cell death by sub-G1 DNA suggested an apoptosis induction following *EZH2* or *MYC* knockdown in combination with IFN-γ treatment in DU145, but not LNCaP, cells (Figure 4F). Crucially, the enhanced apoptosis induced by the combination conditions was IFNGR1 dependent, as the addition of a specific IFNGR1-neutralizing antibody, CD119, which presumably blocks binding of the IFN-γ ligand to IFNGR1, almost completely abolished the apoptosis induced upon EZH2 or MYC knockdown (Figure 4F).

Because EZH2 has been linked to cancer stemness (Sparmann and van Lohuizen, 2006), we further assessed the effect of EZH2 knockdown in tumorsphere formation in prostate cancer cells (prostatosphere), a growth feature associated with tumor-initiating cells (Crea et al., 2011; Duhagon et al., 2010). As shown in Figure 4G, EZH2 knockdown in combination with IFN-γ efficiently inhibited tumorsphere formation in MYC-dependent DU145 and PC3 cells, but not in MYC-independent LNCaP and 22RV1 cells (Figure 4G). Taken together, these findings support the notion that MYC and EZH2 act concertedly in the same pathway to promote growth and survival through inactivation of the IFN-γ-STAT1 tumor suppressor pathway. Restoration of IFN-γ-STAT1 signaling following *EZH2* knockdown is able to sensitize MYC-dependent prostate cancer cells to IFN-γ treatment.

Pharmacologic Depletion of EZH2 by DZNep Mimics EZH2 Knockdown to Restore *IFNGR1* Expression and Sensitize Cells to IFN-γ Treatment

To demonstrate the translational value of this finding, we next asked whether a therapeutic benefit from restoring IFN signaling could be achieved through a pharmacological approach. To this end, we exploited two types of pharmacologic agents: (1) the histone methylation inhibitor deazaneplanocin A (DZNep), which is not specific but is able to effectively deplete EZH2/PRC2, leading to activation of EZH2 target genes (Tan et al., 2007), and (2) the recently reported catalytic inhibitors of EZH2, which can specifically inhibit H3K27me3 but do not affect EZH2 expression (Knutson et al., 2012; McCabe et al., 2012b; Qi et al., 2012). The results show that pharmacological depletion of EZH2 by DZNep in DU145 cells was able to mimic *EZH2* knockdown and induced the expression of *IFNGR1*, which when combined with IFN-γ led to strong inductions of IFN genes (Figure 5A) as well as STAT1 phosphorylation (Figure 5B). Again, in agreement with the selective repression of *IFNGR1* by EZH2, DZNep treatment did not change *IFNAR1* expression (Figures 5A and 5B).

Like EZH2 knockdown, DZNep was able to induce robust apoptosis when combined with increasing doses of IFN-γ in DU145, but not LnCap, cells (Figure 5C). Similarly, consistent with the MYC dependency, such an induction of apoptosis was only seen in RWPE1-MYC cells, and not in RWPE1-PI3K or control RWPE cells (Figure S3A). For comparison, we also show that the other epigenetic compounds (e.g., the histone deacetylase inhibitors SAHA and TSA, and the DNA methylation inhibitor 5′Aza) did not give rise to such a response (Figure S3B), underscoring the unique ability of DZNep in this scenario. Again, the apoptosis induced by the drug combination was inhibited by the neutralizing antibody (CD119) of the IFN-γ receptor (Figure 5D), which was accompanied by the abolished induction of STAT1 phosphorylation and PARP cleavage (Figure 5E). We also show that Axon 1588, a small-molecule inhibitor of JAK2, could similarly rescue DU145 cells from apoptosis (Figure S3C). Taken together, these findings demonstrate that the apoptosis induced by the combination of DZNep and IFN-γ is largely mediated through the specific activation of IFN-γ-STAT1 signaling pathway.

Moreover, the cotreatment of DZNep and IFN-γ was also able to show a combinatorial effect on growth inhibition in MYC-dependent DU145 and PC3 cells, but not in MYC-independent LNCaP and 22RV1 cells (Figure 5F). Most strikingly, this combination almost completely eliminated the formation of DU145 or PC3-derived prostatospheres, but had no effect on LNCaP- or 22RV1-derived prostatospheres (Figure 5G). Consistently, we detected a drastic increase in the expression of *IFN* genes in DU145 prostatospheres upon the combination treatment (Figure S3D). These findings indicate that DZNep is able to recapitulate the *EZH2* knockdown and synergize with IFN-γ to induce apoptosis, cell proliferation, and tumorsphere inhibition in MYC-dependent prostate cancer cells.

Therapeutic Effect of Combined DZNep and IFN-γ Treatment In Vivo

To confirm the above findings in vivo, we established DU145 xenografts in athymic mice and treated them with vehicle, DZNep, IFN-γ, or both DZNep and IFN-γ. Treatment with DZNep

(D) Pearson correlation analysis between MYC and IFNGR1 protein levels of the TMA performed in (C) as represented by the Pearson R score (R < 0 denotes negative correlation). The prostate tumors are stratified into low-grade tumors (≤ stage II, Gleason score < 7, n = 14) and high-grade tumors (stages III and IV, Gleason score ≥ 7, n = 66).

(E) Prostate tumors are stratified into low-grade tumors and a subset of high-grade tumors with high MYC and EZH2 protein expression (n = 20). High-MYC and -EZH2 prostate tumors are defined as high-grade tumors with MYC and EZH2 H-score above their respective median expression.

(F) Representative images of the prostate cancer TMA-IHC staining showing the downregulation of IFNGR1 in advanced prostate cancer tumors with high levels of EZH2 and MYC. Scale bars, 100 μm.

Unless stated otherwise, *p < 0.05, **p < 0.01, ***p < 0.001, n.s., not significant.

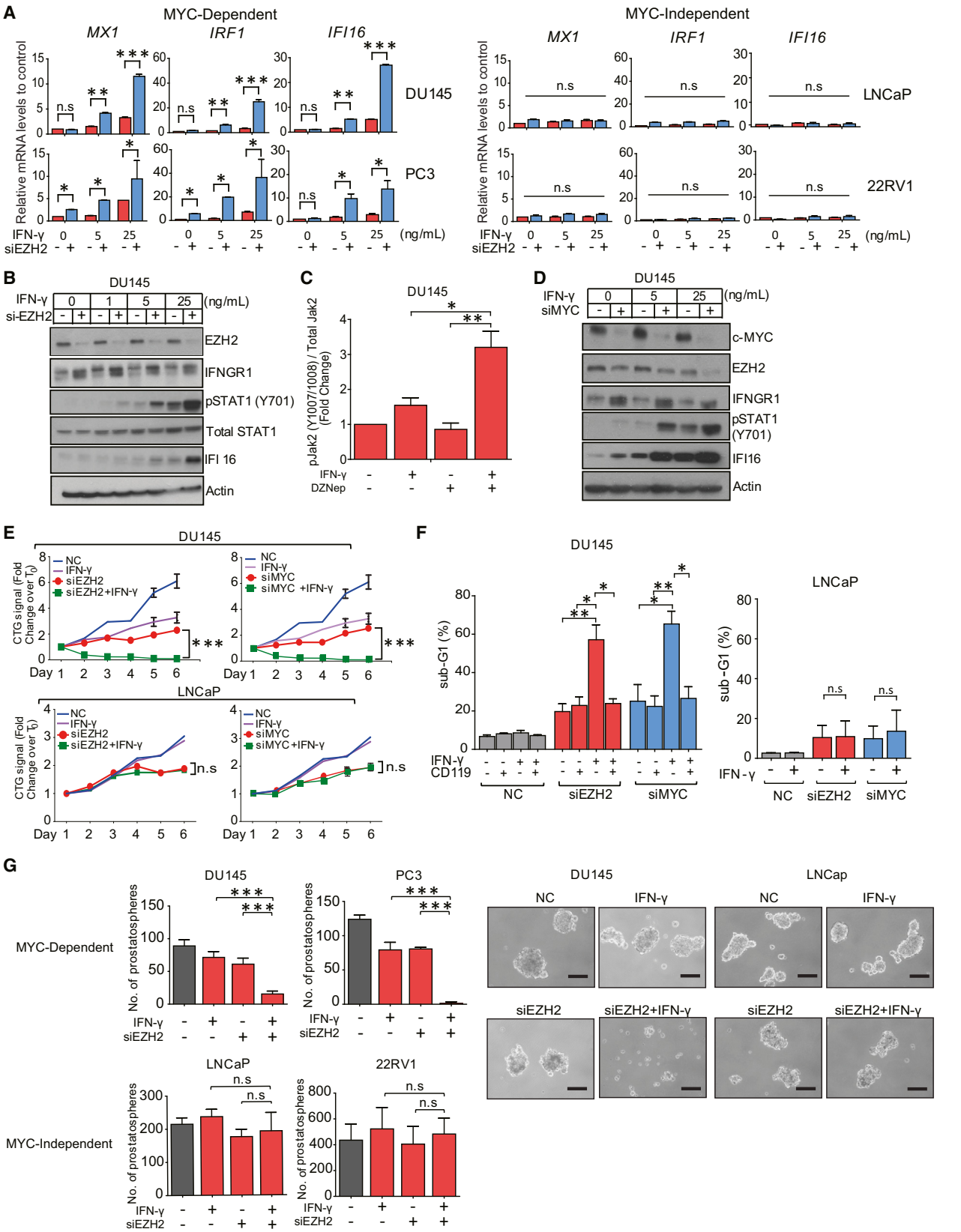

(legend on next page)

or IFN-γ alone slowed down the tumor growth, while the combination treatment resulted in complete tumor growth arrest on average ($p < 0.01$; Figure 6A) and a few of these tumors showed tumor repression (data not shown). Throughout the study, both single and combination treatments were well tolerated in mice without overt signs of toxicity or weight loss of >10%, supporting the potential application of this treatment in the clinic (Figure 6B). IHC analyses of tumors resected from the mice confirmed the downregulation of EZH2 and upregulation of IFNGR1 within the tumors treated with DZNep or DZNep combined with IFN-γ (Figure 6C). Thus, the combination of DZNep and IFN-γ was also effective in the xenograft tumor model and was able to induce the expected molecular changes within the tumors. Collectively, our data demonstrate a therapeutic approach that may be beneficial for advanced prostate cancers that undergo EZH2-mediated IFNGR1 silencing.

Catalytic Inhibitors of EZH2 Fail to Recapitulate the EZH2 Knockdown Effects

Next, we wanted to test whether the catalytic EZH2 inhibitors that were recently developed to selectively inhibit EZH2-mediated H3K27me3 and kill non-Hodgkin's lymphomas harboring EZH2-activating mutations (Knutson et al., 2012; McCabe et al., 2012b; Qi et al., 2012; Verma et al., 2012) are able to mimic the EZH2 knockdown. As shown in Figure 7A, DU145 cells treated with such an EZH2 inhibitor (GSK343) at doses of up to 2.5 μM for 3 days did not show an induction of IFNGR1, despite the efficient depletion of H3K27me3 to as low as 0.1 μM. Cells treated with another EZH2 inhibitor, GSK126, at higher doses (up to 10 μM) for 10 days showed only a modest induction of IFNGR1 (Figures 7A and 7B). In contrast, DZNep, which depleted EZH2, as well as two other PRC2 proteins (EED and SUZ12), induced a marked expression of IFNGR1, but showed a much lower efficiency in depleting H3K27me3 (Figures 7A and 7B). At the *IFNGR1* gene-promoter level, we saw that DZNep treatment reduced both EZH2 and H3K27me3 enrichments, although GSK126 depleted H3K27me3 more efficiently (Figure 7C). In contrast, other repressive histone marks, such as H3K9me3 and H3K9me2, were not affected by DZNep or GSK126 treatment (Figure S4A). Moreover, in addition to *IFNGR1*, the two other known EZH2 targets, *ADRB2* and *DABIP2*, were induced only by DZNep, and not by GSK343 (Figure S4B), suggesting that the inability of the catalytic inhibitors of EZH2 to induce EZH2 target gene expression is not restricted to *IFNGR1*. Accordingly, unlike the DZNep and IFN-γ treatment, GSK343 or GSK126 in combination with IFN-γ failed to induce apoptosis in DU145 cells treated for either 3 days or 10 days (Figure 7D). Moreover, the GSK126 and IFN-γ combination was also unable to inhibit DU145 tumorsphere formation (Figure 7E). Taken together, these findings suggest that although H3K27me3 has been thought of as a repressive histone hallmark associated with PRC2 activity, simply inhibiting H3K27me3 without affecting PRC2 abundance is insufficient to induce *IFNGR1* expression and thus is unable to mimic *EZH2* knockdown. Therefore, additional mechanisms might be required to coordinate with H3K27me3 to implement PRC2-mediated *IFNGR1* silencing in the absence of gain-of-function EZH2 mutations in epithelial tumors. This result is consistent with a very recent report showing that a peptide that blocks EZH2-EED binding, which leads to EZH2 downregulation, is able to induce the loss of cell viability in solid tumor cells, whereas GSK126 is unable to do so despite its high potency in inhibiting H3K27me3 (Kim et al., 2013b).

DISCUSSION

By analyzing the MYC-mediated transcriptional alteration in prostate cancer cells, we uncovered a defective IFN-JAK-STAT1 signaling pathway that is inactivated by EZH2 in a MYC-dependent manner. We show that the direct silencing of *IFNGR1* by EZH2 mediates the inactivation of this pathway, rendering the cancer cells insensitive to IFN-γ treatment. As such, restoration of *IFNGR1* expression by EZH2 inhibition, through gene knockdown or pharmacologic depletion, sensitizes IFN-γ to activate the downstream STAT1 tumor-suppressor pathway, leading to robust apoptosis. We show that this scenario is MYC dependent, which is consistent with MYC being an upstream regulator of EZH2 (Kaur and Cole, 2013; Koh et al., 2011; Sander et al., 2008). In contrast, EZH2 gene-silencing activity may be antagonized by PI3K-AKT signaling through inhibitory EZH2 phosphorylation on serine 21 (Cha et al., 2005; Kaur and Cole, 2013). Indeed, *MYC* knockdown mirrors *EZH2* knockdown, and MYC is required for EZH2 and H3K27me3 enrichment at the *IFNGR1* promoter. We further show that *IFNGR1* downregulation is evident in a subset of advanced prostate tumors where it inversely correlates with *MYC* and *EZH2* expression. Thus, given that MYC is overexpressed in up to 30% of advanced prostate cancer (Koh et al., 2010; Sato et al., 1999) and that MYC overexpression confers

Figure 4. MYC/EZH2-Mediated Inactivation of IFN-γ-JAK-STAT1 Signaling Confers Growth and Survival Advantages

(A) qRT-PCR analysis of three IFN-responsive genes (MX1, IRF1, and IFI16) in DU145, PC3, LNCaP, and 22RV1 cells.

(B) Western blot analysis of IFNGR1 expression and IFN-γ signaling upon EZH2 knockdown in the presence of IFN-γ at the doses as indicated.

(C) ELISA showing JAK2 phosphorylation and activation in DU145 cells treated with siEZH2, IFN-γ, (25 ng/mL), or both. The Y1007/1008 phosphorylation level of JAK2 was normalized and expressed as the fold change against the total JAK2 level.

(D) Western blot analysis of IFNGR1 expression and IFN-γ signaling upon MYC knockdown in the presence of IFN-γ at the indicted doses.

(E) Cell proliferation assay in DU145 and LNCaP cells treated with either siMYC or siEZH2 in combination with IFN-γ. The proliferation of the cells is represented as the fold change after normalizing to the baseline Cell Titer Glow (CTG) signal on day 0 (T_0). All of the data in the graphs represent mean ± SEM, n = 3.

(F) Left: sub-G1 DNA assessment by fluorescence-activated cell sorting (FACS) in DU145 cells treated with siEZH2 or siMYC together with IFN-γ, in the presence or absence of CD119, the IFNGR1 neutralizing antibody. Right: sub-G1 DNA analysis by FACS in LnCap cells treated with siMYC or siEZH2 in combination with IFN-γ.

(G) Left: prostatosphere formation assay after treatment of DU145, PC3, LNCaP, and 22RV1 with either IFN-γ, siEZH2, or both for 7 days. Right: representative phase-contrast microscopy images of the prostatospheres at 10× magnification after treatment with siEZH2 and IFN-γ (25 ng/mL). Scale bars, 100 μm.

Unless stated otherwise, all of the data in the graphs represent mean +SEM, n = 3. *$p < 0.05$, **$p < 0.01$, ***$p < 0.001$, n.s., not significant.

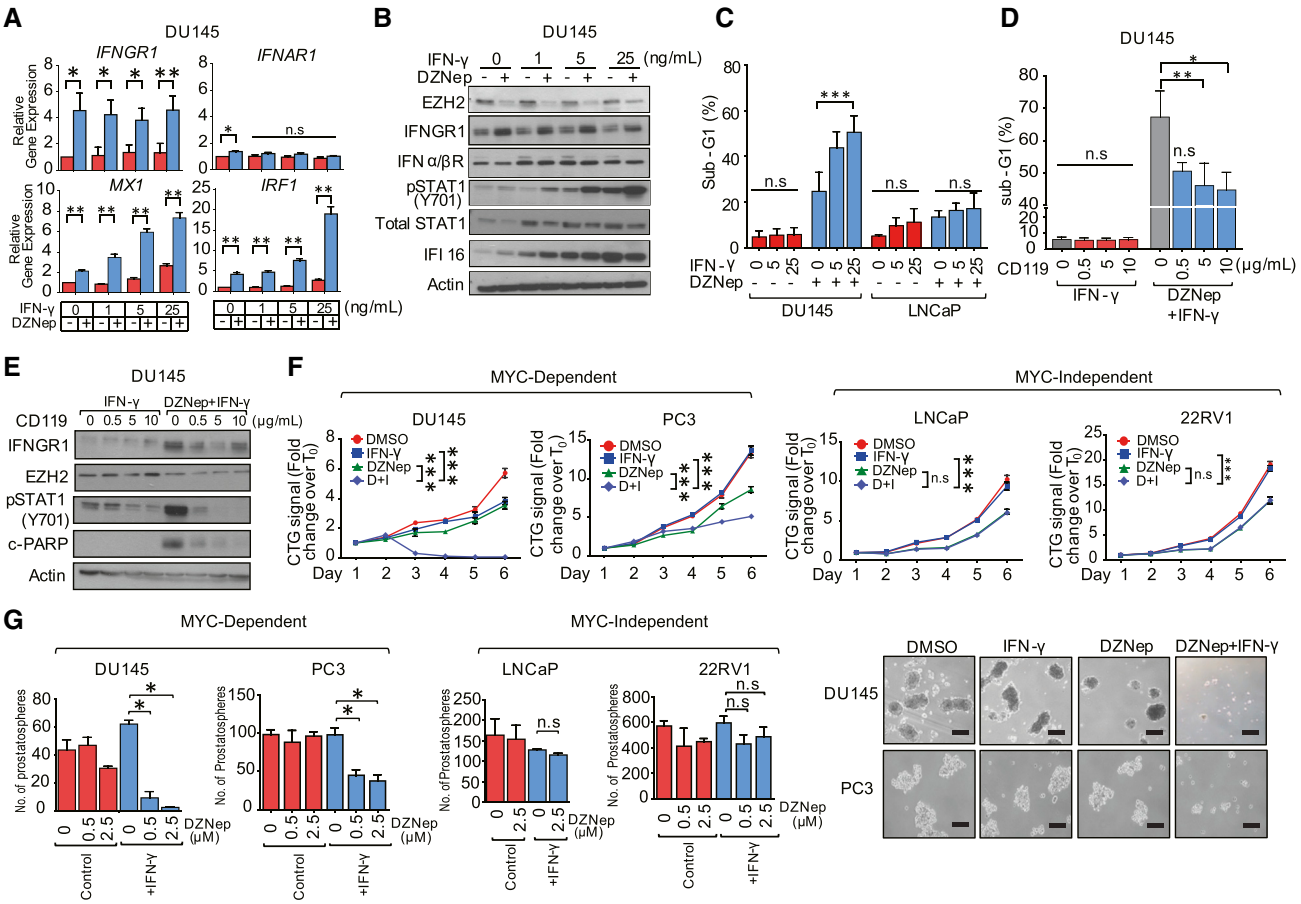

Figure 5. DZNep Mimics EZH2 Knockdown to Restore IFN-γ Response for Growth Inhibition and Apoptosis

(A) qPCR showing the increase in gene expression of *IFNGR1* and various IFN-responsive genes, but not *IFNAR1*, after 72 hr of DZNep (2.5 μM) and IFN-γ treatment at the indicated doses.

(B) Western blot analysis of IFNGR1 expression and IFN-γ signaling in DU145 cells treated with DZNep (2.5 μM), IFN-γ, or both for 3 days.

(C) Sub-G1 DNA analysis in DU145 and LNCaP cells treated as in (B).

(D) Sub-G1 DNA analysis in DU145 cells treated with DZNep/IFN-γ as above in the presence or absence of the IFNGR1-neutralizing antibody CD119 at the indicated concentrations.

(E) Western blot analysis of EZH2, IFN signaling, and PARP cleavage in DU145 cells treated with DZNep and IFN-γ under similar conditions as in (D).

(F) Cell proliferation assay of MYC-dependent cell lines (DU145 and PC3) and MYC-independent cell lines (LNCaP and 22RV1) after treatment with IFN-γ, DZNep, or both for days as indicated. The proliferation of the cells is represented as the fold change after normalizing to the baseline CTG signal on day 0 (T_0).

(G) Left: prostatosphere formation assay showing the effectiveness of combining low doses of DZNep with IFN-γ to inhibit the formation of prostatospheres in the indicated cell lines. Right: representative phase-contrast microscopy images of the prostatospheres of DU145 and PC3 taken at 10× magnification after treatment with DZNep (0.5 μM) and IFN-γ (25 ng/mL). Scale bars, 100 μm.

All of the data in the graph bars represent mean + SEM, n = 3. *p < 0.05, **p < 0.01, ***p < 0.001, n.s., not significant. See also Figure S3.

androgen independency (Bernard et al., 2003) and metastasis (Bernard et al., 2003; Wolfer and Ramaswamy, 2011), these findings support a potential clinical application for context-dependent targeting of MYC-associated refractory prostate cancer, for which there is currently a lack of effective therapy.

From a therapeutic point of view, our approach demonstrated the ability of EZH2-targeted therapy to reconstitute a pathway dependency that drives drug susceptibility. IFN-γ has previously been used to treat advanced prostate cancer, with disappointing results (Bulbul et al., 1986; Hastie, 2008). Although the reason for this is unknown, our findings suggest that the downregulation of *IFNGR1* might provide a possible explanation for the lack of efficacy of IFN-γ treatment. Thus, the combination approach we identified in this study might have the potential to improve IFN-γ treatment in advanced prostate cancer. We found that a subtoxic low dose of DZNep and IFN-γ induced synergistic antitumor activity in the DU145 xenograft model, but did not result in any overt toxicity in the mice. In fact, we did not observed any body weight loss with the use of DZNep even when it was administered together with IFN-γ daily for up to 5 weeks. Although DZNep is not an EZH2-H3K27me3-specific inhibitor and may affect additional histone methylations or other targets, the remarkable similarity between the results produced by RNAi-mediated or chemical inhibition strongly suggests that

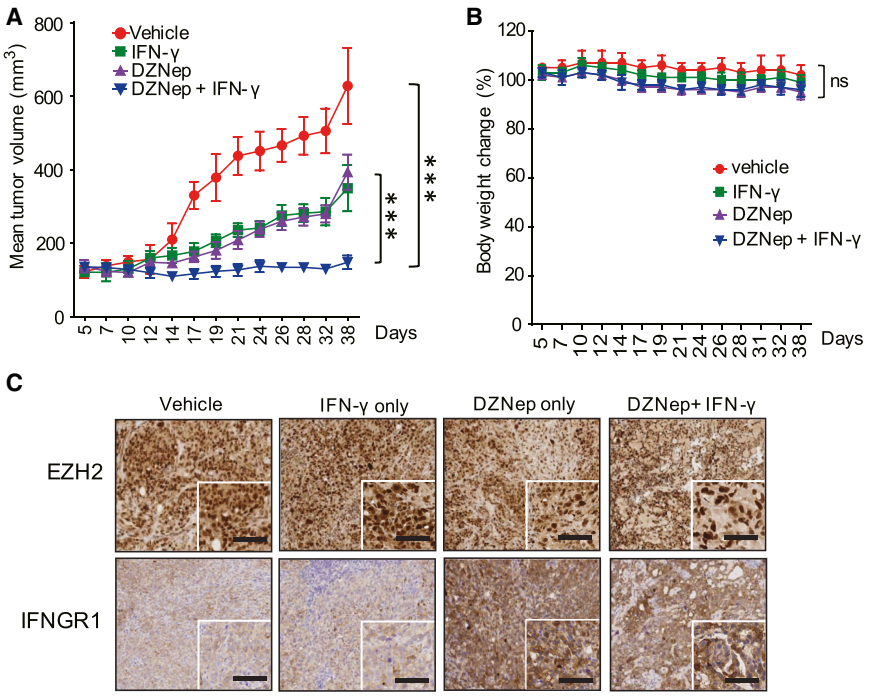

Figure 6. Combinatorial Antitumor Effects of DZNep and IFN-γ In Vivo

(A) DU145 xenograft tumor growth in male athymic nude mice treated with vehicle (n = 5), IFN-γ (1 × 10^7 IU/kg, i.p.; n = 6), DZNep (1 mg/kg, s.c.; n = 7), or both (n = 8). Mean tumor volume ± SEM is shown; ***p < 0.001.

(B) Body weight change (± SEM) during the drug treatment.

(C) IHC analysis of EZH2 and IFNGR1 expression in tissue sections taken from DU145 xenograft tumors after the treatment in (A). Insets are zoomed-in images; scale bars, 100 μm.

DZNep in this scenario acts to recapitulate the *EZH2* knockdown to restore *IFNGR1* expression and thus STAT1 activation. Interestingly, *IFNGR1* suppression by EZH2 may not be restricted to prostate cancer and could occur in other human cancers, such as breast, lung, and liver cancers, as revealed by an Oncomine analysis (data not shown). Thus, it will be interesting to see whether the combination strategy we identified in this study may be applicable to other cancers as well. However, EZH2-mediated *IFNGR1* suppression in other cancer types may not necessarily be linked to MYC overexpression, as MYC expression was weakly correlated with the EZH2 and *IFNGR1* levels in these cancers (data not shown). Thus, the MYC-mediated *EZH2* regulation of *IFNGR1* expression could be cancer specific. Moreover, the levels of *EZH2* and *IFNGR1* expression could potentially be applied as biomarkers in a relevant context, such as advanced prostate cancer, to identify patients who might benefit from the combined EZH2 and IFN-γ-based therapy.

Current efforts to design EZH2-targeted cancer therapies are directed toward therapeutic targeting of H3K27me3. Indeed, small-molecule inhibitors specific for EZH2-mediated H3K27me3 have been reported to be selectively efficacious in lymphomas carrying activating mutations of EZH2 that can cause hyperactive H3K27me3 (Knutson et al., 2012; McCabe et al., 2012b; Qi et al., 2012). To date, activating EZH2 mutations have not been found in epithelial-derived solid tumors; thus, the anticancer activity of the enzymatic inhibitor of EZH2 toward these tumors has yet to be determined. Notably, in breast cancer cells, it has been shown that the EC_{50} for growth inhibition is 200-fold higher than that required to deplete cellular H3K27me3, indicating that inhibiting H3K27me3 alone might be insufficient to recapitulate the cellular effects of *EZH2* knockdown (Verma et al., 2012). Moreover, a recent study showed that a peptide that blocks EZH2-EED interaction can result in EZH2 downregulation and target gene activation, whereas the EZH2 catalytic inhibitor GSK126 is unable to achieve the same, but is much more effective in blocking H3K27me3 (Kim et al., 2013b). Taken together, it seems that disruption of EZH2/PRC2 is required for effective inhibition of EZH2 function in EZH2-overexpressing tumors that do not carry activating mutations of EZH2, which can be achieved by DZNep or a peptide targeting the EZH2-EED interaction, but not by catalytic inhibitors of EZH2. The mechanism for this remains elusive, but one possible scenario is that H3K27me3 may engage additional repressive factors to enforce gene silencing. This idea warrants further investigation.

In addition to the canonical function of EZH2 in gene silencing, recently described "noncanonical" roles of EZH2, independent of histone methylations, such as in activation of NF-κB, AR, or STAT3 signaling, may also contribute to oncogenesis (Lee et al., 2011; Shi et al., 2007; Xu et al., 2012). In particular, in advanced prostate cancer, serine 21 phosphorylation of EZH2 may switch the EZH2 gene-silencing activity to a Polycomb-independent activity (Xu et al., 2012). Thus, we envision a model in which both canonical and noncanonical activities of EZH2 contribute to oncogenesis (Figure 7F). As such, depletion of EZH2, rather than inhibition of H3K27me3 alone, might be necessary for a full phenotypic response. In this regard, IFN-γ-induced IFNGR1-STAT1 activation upon *EZH2* knockdown or DZNep treatment might be one of several crucial mechanisms that contribute to a strong tumor-suppressive response.

EXPERIMENTAL PROCEDURES

Cell Cultures and Treatments

We obtained epithelial cell lines from the American Type Culture Collection and cultured them according to the recommended protocols. Cells were grown to 80% confluence before they were treated with the indicated drugs. Additional details regarding the cell culture methods are provided in Supplemental Experimental Procedures.

Gene-Expression Analysis

Total RNA was isolated with the use ofTrizol (Invitrogen) and purified with the RNeasy Mini Kit (QIAGEN). Microarray hybridization was performed using the

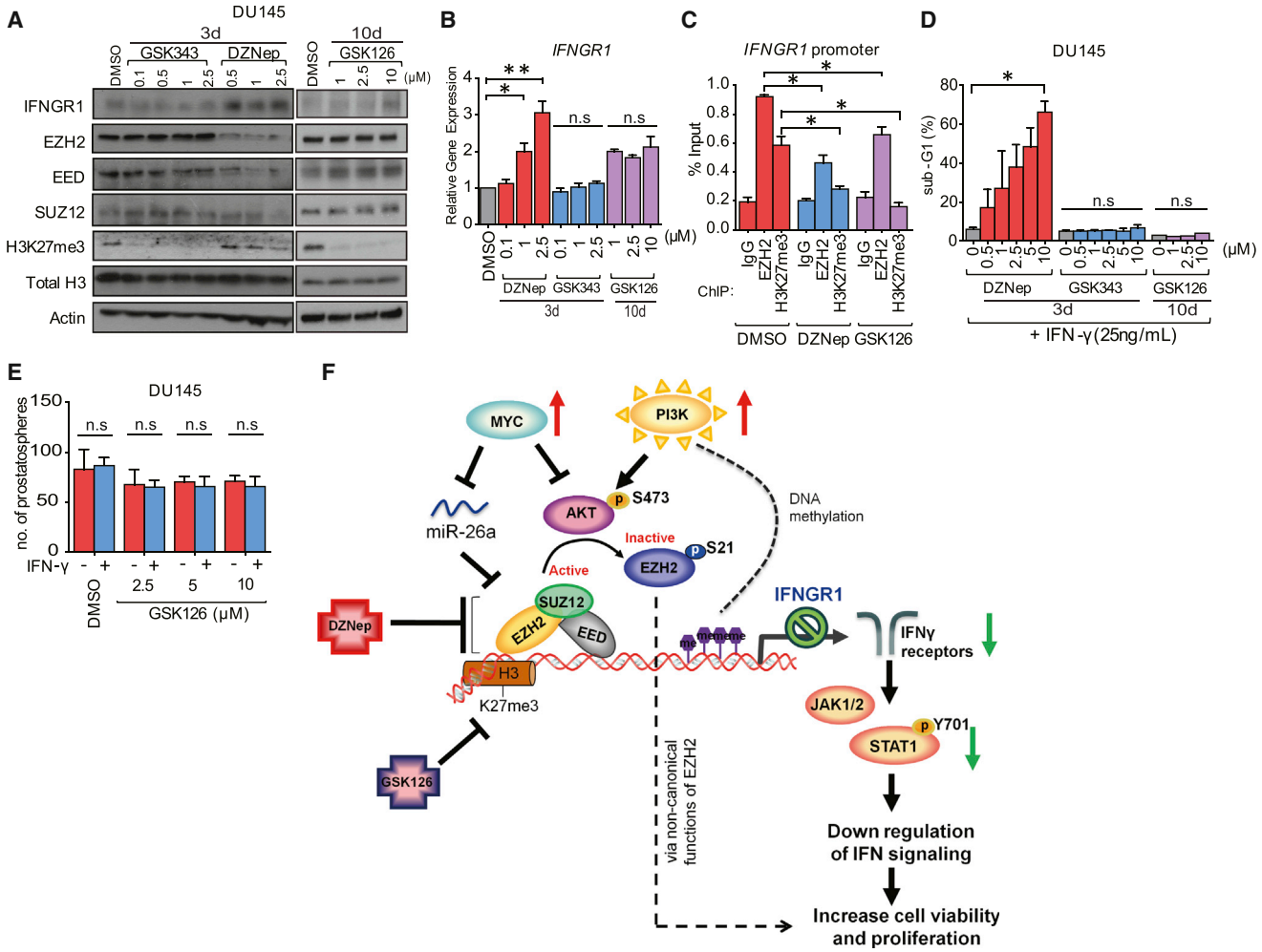

Figure 7. Catalytic Inhibitors of EZH2 Fail to Recapitulate the EZH2 Knockdown Effects

(A) Western blot analysis of IFNGR1, PRC2 proteins, and H3K27me3 in DU145 cells treated with DZNep, GSK343, or GSK126 at the indicated doses for 3 or 10 days.

(B) qRT-PCR analysis of *IFNGR1* expression in DU145 cells treated with the indicated drugs for 3 or 10 days.

(C) ChIP analysis of EZH2 and H3K27me3 enrichments at *IFNGR1* in DU145 cells treated with DMSO, DZNep (2.5 μM), or GSK126 (5 μM) for 3 days. Enrichments were expressed as the percentage of total input used for ChIP.

(D) Sub-G1 DNA analysis in DU145 cells treated with DZNep or GSK343/GSK126 in combination with IFN-γ as indicated.

(E) Prostatosphere-formation assay after treatment of DU145 cells with IFN-γ (25 ng/mL) and GSK126 for 10 days at the indicated doses.

(F) Model for EZH2-mediated inactivation of IFN-JAK-STAT1 signaling regulated by MYC and PI3K-AKT. MYC overexpression leads to EZH2 activation by antagonizing miR-26a and PI3K-AKT-mediated EZH2 inhibition, resulting in suppression of *IFNGR1* and downstream JAK-STAT1 signaling. DZNep depletion of EZH2/PRC2 restores *IFNGR1* expression and synergizes with IFN-γ to induce growth inhibition and apoptosis.

All of the data in the graph bars represent mean + SEM, n = 3. *p < 0.05, **p < 0.01, n.s., not significant. See also Figure S4.

Illumina Gene Expression Sentrix BeadChip HumanRef-8_V3, and data analysis was performed with GeneSpring software (Agilent Technologies) as described previously (Lee et al., 2011). The gene sets analyzed by GeneSpring were next subjected to IPA for Gene Ontology (GO) analysis. Additional assays of transcript abundance to validate the microarray results were performed by qRT-PCR (Supplemental Experimental Procedures).

IHC Analysis

Prostate TMA slides were purchased from US Biomax. Briefly, paraffin-embedded tissue sections (5 μg thick) were cut, deparaffinized, and rehydrated, and antigens were retrieved using Proteinase K solution. The sections were then incubated in 3% H_2O_2 at room temperature to block endogenous peroxidase. The slides were incubated in anti-EZH2 clone D2C9 XP (Cell Signaling), iFNGR1 antibody clone GIR-94 (SCBT), or Myc antibody (SCBT) for 45 min, followed by a 30 min incubation with anti-mouse labeled polymer. Additional details regarding the IHC analysis are provided in Supplemental Experimental Procedures.

Mouse Experiments

For in vivo evaluation of DZNep and IFN-γ treatment, experiments were conducted in compliance with animal protocols approved by the ASTAR-Biopolis Institutional Animal Care and Use Committee of Singapore. DU145 cells (5×10^6) were subcutaneously injected into 6- to 8-week-old male nude mice, followed by treatment with vehicle, IFN-γ (1×10^7 IU/kg) alone, or DZNep

(1 mg/kg) alone or combined DZNep (1 mg/kg) with IFN-γ (1×10^7 IU/kg). IFN-γ was administered by intraperitoneal injection daily, and DZNep was administered by subcutaneous injection on every alternating day over a period of 38 days after the average tumor size reached ~150 mm^3. Tumors were measured by vernier calliper at least twice per week and the tumor volume was calculated with the following formula: V = W × W × L/2. Each xenograft treatment arm comprised five to eight mice. Differences among groups and treatments were determined by ANOVA followed by Student's t test (***$p < 0.001$; n.s., not significant). Error bars represent means ± SEM.

Statistical Analyses

All in vitro experiments were repeated at least three times unless stated otherwise, and data are reported as means + SEM. Differences among groups and treatments were determined by Student's t test and $p \leq 0.05$ was considered significant unless stated otherwise.

Details regarding the methods used are provided in Supplemental Experimental Procedures.

ACCESSION NUMBERS

The Gene Expression Omnibus database accession number for the microarray data reported herein from the comparison against RWPE1-vector, RWPE1-MYC, and RWPE1-PI3K transformed cells (Figure 1A) is GSE43686.

SUPPLEMENTAL INFORMATION

Supplemental Information includes Supplemental Experimental Procedures, four figures, and one table and can be found with this article online at http://dx.doi.org/10.1016/j.celrep.2014.05.045.

AUTHOR CONTRIBUTIONS

Q.Y. conceived and supervised the project. Z.N.W. and Q.Y. designed the experiments and wrote the manuscript. Z.N.W. performed most of the experiments. Z.N.W. and Z.L. performed animal work. S.T.L. and P.L.L. assisted in data acquisition. Y.P.L. provided a critical reading of the manuscript.

ACKNOWLEDGMENTS

We thank the members of the Histopathology Department of the Institute of Molecular and Cell Biology, A*STAR for their service in IHC staining and analysis. We thank M.Y. Aau for the array hybridization. This work was supported by the A*STAR of Singapore, and Z.N.W. is supported by a scholarship from the National University of Singapore Graduate School for Integrative Sciences and Engineering.

Received: October 17, 2013
Revised: March 4, 2014
Accepted: May 22, 2014
Published: June 19, 2014

REFERENCES

Bachmann, I.M., Halvorsen, O.J., Collett, K., Stefansson, I.M., Straume, O., Haukaas, S.A., Salvesen, H.B., Otte, A.P., and Akslen, L.A. (2006). EZH2 expression is associated with high proliferation rate and aggressive tumor subgroups in cutaneous melanoma and cancers of the endometrium, prostate, and breast. J. Clin. Oncol. *24*, 268–273.

Bernard, D., Pourtier-Manzanedo, A., Gil, J., and Beach, D.H. (2003). Myc confers androgen-independent prostate cancer cell growth. J. Clin. Invest. *112*, 1724–1731.

Bracken, A.P., Pasini, D., Capra, M., Prosperini, E., Colli, E., and Helin, K. (2003). EZH2 is downstream of the pRB-E2F pathway, essential for proliferation and amplified in cancer. EMBO J. *22*, 5323–5335.

Bryant, R.J., Cross, N.A., Eaton, C.L., Hamdy, F.C., and Cunliffe, V.T. (2007). EZH2 promotes proliferation and invasiveness of prostate cancer cells. Prostate *67*, 547–556.

Bulbul, M.A., Huben, R.P., and Murphy, G.P. (1986). Interferon-beta treatment of metastatic prostate cancer. J. Surg. Oncol. *33*, 231–233.

Cao, Q., Yu, J., Dhanasekaran, S.M., Kim, J.H., Mani, R.S., Tomlins, S.A., Mehra, R., Laxman, B., Cao, X., Yu, J., et al. (2008). Repression of E-cadherin by the polycomb group protein EZH2 in cancer. Oncogene *27*, 7274–7284.

Cha, T.L., Zhou, B.P., Xia, W., Wu, Y., Yang, C.C., Chen, C.T., Ping, B., Otte, A.P., and Hung, M.C. (2005). Akt-mediated phosphorylation of EZH2 suppresses methylation of lysine 27 in histone H3. Science *310*, 306–310.

Chang, C.J., and Hung, M.C. (2012). The role of EZH2 in tumour progression. Br. J. Cancer *106*, 243–247.

Crea, F., Hurt, E.M., Mathews, L.A., Cabarcas, S.M., Sun, L., Marquez, V.E., Danesi, R., and Farrar, W.L. (2011). Pharmacologic disruption of Polycomb Repressive Complex 2 inhibits tumorigenicity and tumor progression in prostate cancer. Mol. Cancer *10*, 40.

Duhagon, M.A., Hurt, E.M., Sotelo-Silveira, J.R., Zhang, X., and Farrar, W.L. (2010). Genomic profiling of tumor initiating prostatospheres. BMC Genomics *11*, 324.

Gazin, C., Wajapeyee, N., Gobeil, S., Virbasius, C.M., and Green, M.R. (2007). An elaborate pathway required for Ras-mediated epigenetic silencing. Nature *449*, 1073–1077.

Gonzalez, M.E., Li, X., Toy, K., DuPrie, M., Ventura, A.C., Banerjee, M., Ljungman, M., Merajver, S.D., and Kleer, C.G. (2009). Downregulation of EZH2 decreases growth of estrogen receptor-negative invasive breast carcinoma and requires BRCA1. Oncogene *28*, 843–853.

Grasso, C.S., Wu, Y.M., Robinson, D.R., Cao, X., Dhanasekaran, S.M., Khan, A.P., Quist, M.J., Jing, X., Lonigro, R.J., Brenner, J.C., et al. (2012). The mutational landscape of lethal castration-resistant prostate cancer. Nature *487*, 239–243.

Gurel, B., Iwata, T., Koh, C.M., Jenkins, R.B., Lan, F., Van Dang, C., Hicks, J.L., Morgan, J., Cornish, T.C., Sutcliffe, S., et al. (2008). Nuclear MYC protein overexpression is an early alteration in human prostate carcinogenesis. Mod. Pathol. *21*, 1156–1167.

Hastie, C. (2008). Interferon gamma, a possible therapeutic approach for late-stage prostate cancer? Anticancer Res. *28* (5B), 2843–2849.

Jenkins, R.B., Qian, J., Lieber, M.M., and Bostwick, D.G. (1997). Detection of c-myc oncogene amplification and chromosomal anomalies in metastatic prostatic carcinoma by fluorescence in situ hybridization. Cancer Res. *57*, 524–531.

Kaur, M., and Cole, M.D. (2013). MYC acts via the PTEN tumor suppressor to elicit autoregulation and genome-wide gene repression by activation of the Ezh2 methyltransferase. Cancer Res. *73*, 695–705.

Kim, E., Kim, M., Woo, D.H., Shin, Y., Shin, J., Chang, N., Oh, Y.T., Kim, H., Rheey, J., Nakano, I., et al. (2013a). Phosphorylation of EZH2 activates STAT3 signaling via STAT3 methylation and promotes tumorigenicity of glioblastoma stem-like cells. Cancer Cell *23*, 839–852.

Kim, W., Bird, G.H., Neff, T., Guo, G., Kerenyi, M.A., Walensky, L.D., and Orkin, S.H. (2013b). Targeted disruption of the EZH2-EED complex inhibits EZH2-dependent cancer. Nat. Chem. Biol. *9*, 643–650.

Kleer, C.G., Cao, Q., Varambally, S., Shen, R., Ota, I., Tomlins, S.A., Ghosh, D., Sewalt, R.G., Otte, A.P., Hayes, D.F., et al. (2003). EZH2 is a marker of aggressive breast cancer and promotes neoplastic transformation of breast epithelial cells. Proc. Natl. Acad. Sci. USA *100*, 11606–11611.

Knutson, S.K., Wigle, T.J., Warholic, N.M., Sneeringer, C.J., Allain, C.J., Klaus, C.R., Sacks, J.D., Raimondi, A., Majer, C.R., Song, J., et al. (2012). A selective inhibitor of EZH2 blocks H3K27 methylation and kills mutant lymphoma cells. Nat. Chem. Biol. *8*, 890–896.

Kodach, L.L., Jacobs, R.J., Heijmans, J., van Noesel, C.J., Langers, A.M., Verspaget, H.W., Hommes, D.W., Offerhaus, G.J., van den Brink, G.R., and Hardwick, J.C. (2010). The role of EZH2 and DNA methylation in the silencing

of the tumour suppressor RUNX3 in colorectal cancer. Carcinogenesis *31*, 1567–1575.

Koh, C.M., Bieberich, C.J., Dang, C.V., Nelson, W.G., Yegnasubramanian, S., and De Marzo, A.M. (2010). MYC and prostate cancer. Genes Cancer *1*, 617–628.

Koh, C.M., Iwata, T., Zheng, Q., Bethel, C., Yegnasubramanian, S., and De Marzo, A.M. (2011). Myc enforces overexpression of EZH2 in early prostatic neoplasia via transcriptional and post-transcriptional mechanisms. Oncotarget *2*, 669–683.

Kondo, Y., Shen, L., Cheng, A.S., Ahmed, S., Boumber, Y., Charo, C., Yamochi, T., Urano, T., Furukawa, K., Kwabi-Addo, B., et al. (2008). Gene silencing in cancer by histone H3 lysine 27 trimethylation independent of promoter DNA methylation. Nat. Genet. *40*, 741–750.

Lee, S.T., Li, Z., Wu, Z., Aau, M., Guan, P., Karuturi, R.K., Liou, Y.C., and Yu, Q. (2011). Context-specific regulation of NF-κB target gene expression by EZH2 in breast cancers. Mol. Cell *43*, 798–810.

Li, H., Bitler, B.G., Vathipadiekal, V., Maradeo, M.E., Slifker, M., Creasy, C.L., Tummino, P.J., Cairns, P., Birrer, M.J., and Zhang, R. (2012). ALDH1A1 is a novel EZH2 target gene in epithelial ovarian cancer identified by genome-wide approaches. Cancer Prev. Res. (Phila.) *5*, 484–491.

Luoto, K.R., Meng, A.X., Wasylishen, A.R., Zhao, H., Coackley, C.L., Penn, L.Z., and Bristow, R.G. (2010). Tumor cell kill by c-MYC depletion: role of MYC-regulated genes that control DNA double-strand break repair. Cancer Res. *70*, 8748–8759.

Majumder, P.K., and Sellers, W.R. (2005). Akt-regulated pathways in prostate cancer. Oncogene *24*, 7465–7474.

Margueron, R., and Reinberg, D. (2011). The Polycomb complex PRC2 and its mark in life. Nature *469*, 343–349.

McCabe, M.T., Graves, A.P., Ganji, G., Diaz, E., Halsey, W.S., Jiang, Y., Smitheman, K.N., Ott, H.M., Pappalardi, M.B., Allen, K.E., et al. (2012a). Mutation of A677 in histone methyltransferase EZH2 in human B-cell lymphoma promotes hypertrimethylation of histone H3 on lysine 27 (H3K27). Proc. Natl. Acad. Sci. USA *109*, 2989–2994.

McCabe, M.T., Ott, H.M., Ganji, G., Korenchuk, S., Thompson, C., Van Aller, G.S., Liu, Y., Graves, A.P., Della Pietra, A., 3rd, Diaz, E., et al. (2012b). EZH2 inhibition as a therapeutic strategy for lymphoma with EZH2-activating mutations. Nature *492*, 108–112.

Melnick, A. (2012). Epigenetic therapy leaps ahead with specific targeting of EZH2. Cancer Cell *22*, 569–570.

Morin, R.D., Johnson, N.A., Severson, T.M., Mungall, A.J., An, J., Goya, R., Paul, J.E., Boyle, M., Woolcock, B.W., Kuchenbauer, F., et al. (2010). Somatic mutations altering EZH2 (Tyr641) in follicular and diffuse large B-cell lymphomas of germinal-center origin. Nat. Genet. *42*, 181–185.

Nikoloski, G., Langemeijer, S.M., Kuiper, R.P., Knops, R., Massop, M., Tönnissen, E.R., van der Heijden, A., Scheele, T.N., Vandenberghe, P., de Witte, T., et al. (2010). Somatic mutations of the histone methyltransferase gene EZH2 in myelodysplastic syndromes. Nat. Genet. *42*, 665–667.

Park, S.Y., Seol, J.W., Lee, Y.J., Cho, J.H., Kang, H.S., Kim, I.S., Park, S.H., Kim, T.H., Yim, J.H., Kim, M., et al. (2004). IFN-gamma enhances TRAIL-induced apoptosis through IRF-1. Eur. J. Biochem. *271*, 4222–4228.

Popovic, R., and Licht, J.D. (2012). Emerging epigenetic targets and therapies in cancer medicine. Cancer Discov. *2*, 405–413.

Qi, W., Chan, H., Teng, L., Li, L., Chuai, S., Zhang, R., Zeng, J., Li, M., Fan, H., Lin, Y., et al. (2012). Selective inhibition of Ezh2 by a small molecule inhibitor blocks tumor cells proliferation. Proc. Natl. Acad. Sci. USA *109*, 21360–21365.

Ren, G., Baritaki, S., Marathe, H., Feng, J., Park, S., Beach, S., Bazeley, P.S., Beshir, A.B., Fenteany, G., Mehra, R., et al. (2012). Polycomb protein EZH2 regulates tumor invasion via the transcriptional repression of the metastasis suppressor RKIP in breast and prostate cancer. Cancer Res. *72*, 3091–3104.

Sander, S., Bullinger, L., Klapproth, K., Fiedler, K., Kestler, H.A., Barth, T.F., Möller, P., Stilgenbauer, S., Pollack, J.R., and Wirth, T. (2008). MYC stimulates EZH2 expression by repression of its negative regulator miR-26a. Blood *112*, 4202–4212.

Sato, K., Qian, J., Slezak, J.M., Lieber, M.M., Bostwick, D.G., Bergstralh, E.J., and Jenkins, R.B. (1999). Clinical significance of alterations of chromosome 8 in high-grade, advanced, nonmetastatic prostate carcinoma. J. Natl. Cancer Inst. *91*, 1574–1580.

Shi, B., Liang, J., Yang, X., Wang, Y., Zhao, Y., Wu, H., Sun, L., Zhang, Y., Chen, Y., Li, R., et al. (2007). Integration of estrogen and Wnt signaling circuits by the polycomb group protein EZH2 in breast cancer cells. Mol. Cell. Biol. *27*, 5105–5119.

Sneeringer, C.J., Scott, M.P., Kuntz, K.W., Knutson, S.K., Pollock, R.M., Richon, V.M., and Copeland, R.A. (2010). Coordinated activities of wild-type plus mutant EZH2 drive tumor-associated hypertrimethylation of lysine 27 on histone H3 (H3K27) in human B-cell lymphomas. Proc. Natl. Acad. Sci. USA *107*, 20980–20985.

Sparmann, A., and van Lohuizen, M. (2006). Polycomb silencers control cell fate, development and cancer. Nat. Rev. Cancer *6*, 846–856.

Supino, R., Favini, E., Cuccuru, G., Zunino, F., and Scovassi, A.I. (2007). Effect of paclitaxel on intracellular localization of c-Myc and P-c-Myc in prostate carcinoma cell lines. Ann. N Y Acad. Sci. *1095*, 175–181.

Tan, J., Yang, X., Zhuang, L., Jiang, X., Chen, W., Lee, P.L., Karuturi, R.K., Tan, P.B., Liu, E.T., and Yu, Q. (2007). Pharmacologic disruption of Polycomb-repressive complex 2-mediated gene repression selectively induces apoptosis in cancer cells. Genes Dev. *21*, 1050–1063.

Varambally, S., Dhanasekaran, S.M., Zhou, M., Barrette, T.R., Kumar-Sinha, C., Sanda, M.G., Ghosh, D., Pienta, K.J., Sewalt, R.G., Otte, A.P., et al. (2002). The polycomb group protein EZH2 is involved in progression of prostate cancer. Nature *419*, 624–629.

Verma, S.K., Tian, X., LaFrance, L.V., Duquenne, C., Suarez, D.P., Newlander, K.A., Romeril, S.P., Burgess, J.L., Grant, S.W., and Brackley, J.A. (2012). Identification of potent, selective, cell-active inhibitors of the histone lysine methyltransferase EZH2. ACS Med. Chem. Lett. *3*, 1091–1096.

Wolfer, A., and Ramaswamy, S. (2011). MYC and metastasis. Cancer Res. *71*, 2034–2037.

Wolfer, A., Wittner, B.S., Irimia, D., Flavin, R.J., Lupien, M., Gunawardane, R.N., Meyer, C.A., Lightcap, E.S., Tamayo, P., Mesirov, J.P., et al. (2010). MYC regulation of a "poor-prognosis" metastatic cancer cell state. Proc. Natl. Acad. Sci. USA *107*, 3698–3703.

Xu, K., Wu, Z.J., Groner, A.C., He, H.H., Cai, C., Lis, R.T., Wu, X., Stack, E.C., Loda, M., Liu, T., et al. (2012). EZH2 oncogenic activity in castration-resistant prostate cancer cells is Polycomb-independent. Science *338*, 1465–1469.

Yap, D.B., Chu, J., Berg, T., Schapira, M., Cheng, S.W., Moradian, A., Morin, R.D., Mungall, A.J., Meissner, B., Boyle, M., et al. (2011). Somatic mutations at EZH2 Y641 act dominantly through a mechanism of selectively altered PRC2 catalytic activity, to increase H3K27 trimethylation. Blood *117*, 2451–2459.

Yu, J., Cao, Q., Mehra, R., Laxman, B., Yu, J., Tomlins, S.A., Creighton, C.J., Dhanasekaran, S.M., Shen, R., Chen, G., et al. (2007). Integrative genomics analysis reveals silencing of beta-adrenergic signaling by polycomb in prostate cancer. Cancer Cell *12*, 419–431.

Yu, J., Cao, Q., Yu, J., Wu, L., Dallol, A., Li, J., Chen, G., Grasso, C., Cao, X., Lonigro, R.J., et al. (2010). The neuronal repellent SLIT2 is a target for repression by EZH2 in prostate cancer. Oncogene *29*, 5370–5380.